



Journal of Applied and Computational Mechanics



Research Paper

A Study of Curved Louver Fin Configuration for Heat Transfer Enhancement

Kiatbodin Wanglertpanich¹, Patcharakon Siriyothai², Thanathorn Hempijid³,
Chawalit Kittichaikarn⁴

¹ Department of Mechanical Engineering, Faculty of Engineering, Kasetsart University, Bangkok 10900, Thailand, Email: kaitbourdin.w@ku.th

² Department of Mechanical Engineering, Faculty of Engineering, Kasetsart University, Bangkok 10900, Thailand, Email: thanathorn.he@ku.th

³ Department of Mechanical Engineering, Faculty of Engineering, Kasetsart University, Bangkok 10900, Thailand, Email: patcharakorn.si@ku.th

⁴ Department of Mechanical Engineering, Faculty of Engineering, Kasetsart University, Bangkok 10900, Thailand, Email: fengclk@ku.ac.th

Received July 21 2021; Revised November 19 2021; Accepted for publication January 11 2022.

Corresponding author: C. Kittichaikarn (fengclk@ku.ac.th)

© 2022 Published by Shahid Chamran University of Ahvaz

Abstract. Herein, the heat transfer performance of the curved surface of a louvered fin heat exchanger using computational fluid dynamics (CFD) is examined. Four new models are used with curved surfaces in different locations. The air inlet velocity is 1–9 m/s. The air and fin wall temperature remain constant at 300 and 353 K, respectively. The result of the reference flat fin is confirmed with experimental results. The results demonstrate that curved fins changed the airflow path and created vortices. The air tends to flow between louver fins, improving its velocity and enhancing heat transfer. The result from the case that individual fin is close to the middle fin demonstrated that louver fin provides a 15% increase compared to that of the reference. However, when the air inlet velocity is high, the performance evaluation criteria from the case that individual fin is close to the first fin, is the highest, which results in a 1% increase from that of the reference. Therefore, increasing heat transfer can compensate the effect of pressure drop because of vortices in the louver fin domain. This study can be applied to the air conditioning system to increase its efficiency and cut the operation cost down.

Keywords: CFD; Louver Fin; Heat Exchanger; Convective Heat Transfer.

1. Introduction

Microchannel heat exchangers (MCHXs) play an important role in multiple industrial products such as car radiators and air conditioners. Because of their compact structure and high heat transfer performance, MCHXs have been installed in many equipments with space limitations. Unfortunately, MCHXs suffer from a high pressure drop, increasing energy consumption. Mori and Nakayama [1] reported that automotive industries mostly used compact HXs because of limited space. The fin geometry, particularly fin shape, requires to be carefully modified to enhance heat transfer. One of the most compact HXs is a louvered fin, which can be formed using a pressing machine. This allows louvered fins to be more cost effective compared to other flow-interrupted geometries for large-scale production [2].

Multiple experimental investigations demonstrated that heat transfer and pressure drop are correlated [3-7]. Kim and Bullard [8] used water as a coolant flowing in the microchannel tubes. Then, they correlated Colburn j -factor (j) with the Fanning friction factor (f). Both factors depend on the individual geometrical parameter of the louvered fin. However, these correlations can be applied when the ratio of the fin pitch (H) to the louver pitch (L_p) is <1 . Nevertheless, Shah and Sekulic [9] reported that this ratio should have a value of >1 for corrugated louvered fins and reported correlations for $100 < Re < 3000$. They used computational fluid dynamics (CFD) to confirm their numerical results with experiments to confirm these correlations. Furthermore, Sadeghianjahromi et al. [10] numerically examined these correlations and introduced an equation applicable to flat fins (with a louver angle of 0°).

CFD is extensively used to examine and optimize MCHX performance because it requires a relatively short time and the expense for conducting research is lesser. Perrotin and Clodic [11] performed CFD and compared the thermal distributions of 2D and 3D CFD models. Although the 2D model gave more error than the 3D model, it required a shorter time and less computing power in the area that involved fine grids. [12, 13] used CFD to obtain parameter optimization for the louvered fin in an MCHX. Ryu et al. [12] reported that the simulation of a 2D steady flow in the MCHX using a realizable k - ϵ turbulent model led to a 5% error, while that of the 3D steady model led to only a 2% error. Furthermore, the error caused by the 2D model tended to decrease at a high Reynolds number (Re). Qian et al. [14] conducted a study on the influence of the inlet velocity profile on heat performance; however, it seemed difficult to obtain the airflow as assumed.



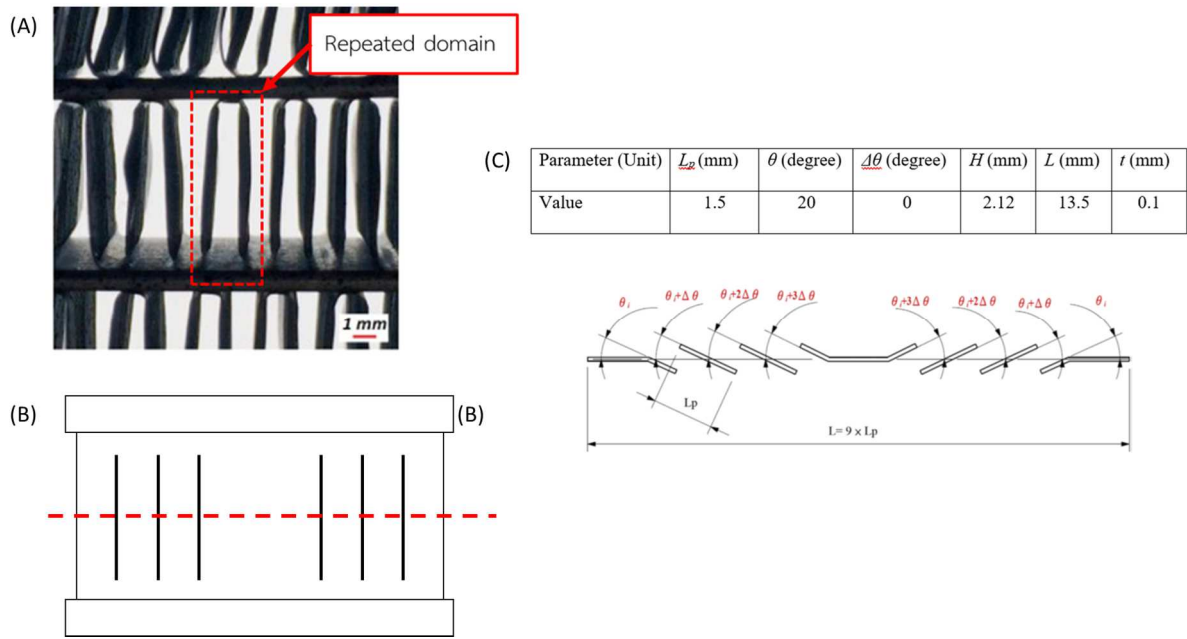


Fig. 1. Geometric parameter of a louver fin from Jang and Chen [13].

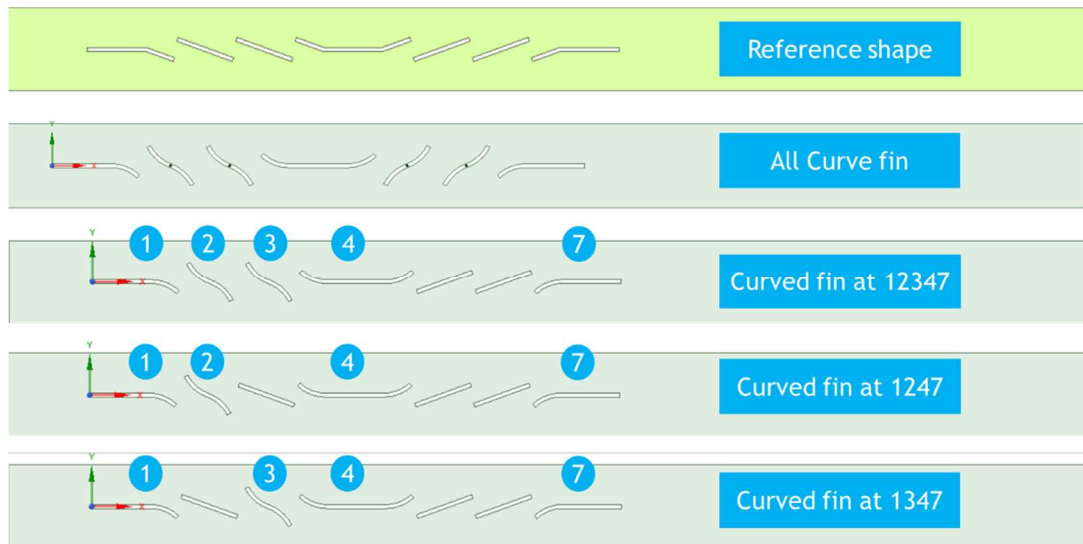


Fig. 2. Five designs labeled using the location of the curved fins.

The standard orientation of the louvered fin array is linear. Certain studies introduced a staggered array to enhance heat transfer. Tanaka et al. [15] varied geometrical parameters of an inclined louvered fin to enhance heat exchanger performance. Manglik and Bergles [16] presented the overview data of an offset fin array with a louver angle fixed at 0°. They used a multi-regression analysis to propose the correlation for both heat transfer and pressure drop in dependence on the fin geometry, the Reynolds number and the Prandtl number. Dejong and Jacobi [17] performed flow visualization and demonstrated that convective heat transfer increased with fins having shedding vortices. Wanglertpanich and Kittichaikarn [18] proposed triangular zigzag louvered fin structure. This geometrical change was able to improve heat transfer efficiency by increasing the time for which air was trapped inside a fin domain. Therefore, change in geometrical parameters of louvered fin altered heat transfer performance.

The effect of louver fin shape variation on heat exchanger performance plays an important role in altering heat transfer in MCHXs. We hypothesized that (1) changing its geometry from the ordinary flat to the curved louver fin could increase its heat transfer performance and (2) the locations of the curved louver fin could affect its heat exchanger performance. We maintained the heat transfer area constant to control the curved fins such that no additional material was required during the manufacturing process. Moreover, this study can be applied to an air conditioning system to increase its efficiency and reduce operational costs.

2. Problem Statement

2.1 Geometrical Configuration

Five designs were performed in this study. The first one was the traditional louver fin. Its parameters were selected based on the study by Jang and Chen [13], validated using an infrared (IR) thermograph. Their geometric dimensions are shown in Fig. 1. This model was used as a reference in this study. The other four designs were modified by changing the ordinary flat surface of the louver fin to a curved shape. The new designs were named by the numbers of curved fins (at 1-2-3-4-7, 1-2-4-7, and 1-3-4-7) except for the reference and all-curved fins (Fig. 2). We used 2D models while 3D models were used in Jang and Chen [13]. Their z+ and z-



planes were symmetric boundary conditions, which were simplified in 2D simulations that yielded the same results. Although the fins were curved, the heat transfer area of the louver fin was kept constant. Fig. 3 shows the curved fin shape with the same fin length as an ordinary flat fin. The radius of curvature was constrained at 1 mm. The first, middle, and last fins were curved at the inclined section, whereas the others were separated into two sections above and below the center. These zones were on the other side of the curvature (shown in Fig. 3). Thus, there was no requirements to add additional material to increase the heat transfer area.

2.2 Computational Domain and Boundary Conditions

A hybrid conformal meshing was indicated in this study. Owing to the fluid flow at the near-wall region and heat transfer from the wall to it, its faces that were in contact with the heated wall were refined by creating thin layers of finer meshes. The first layer thickness y^+ was monitored to be <1 ; the result of meshing is shown in Fig. 4.

To eliminate the effects of the inlet and outlet, the upstream and downstream of the fluid domain were extended 1 and 7 times of the fin pitch (H), respectively. The top and bottom planes of the domain were designated as the periodic boundaries from the flow the left of the domain to the adjacent repetitive domain, and therefore creating a periodic plane reduced several meshes. As shown in Fig. 5, the flow velocity (U_{in}) was assumed to be uniform and constant at 1–9 m/s, and the temperature (T_i) was 300 K at the inlet. The outlet of the domain was outflow, and the gradient of all variables was set to 0. The temperature at the fin surface (T_w) was constant at 353 K. The air and Al properties were then based on ANSYS database [19].

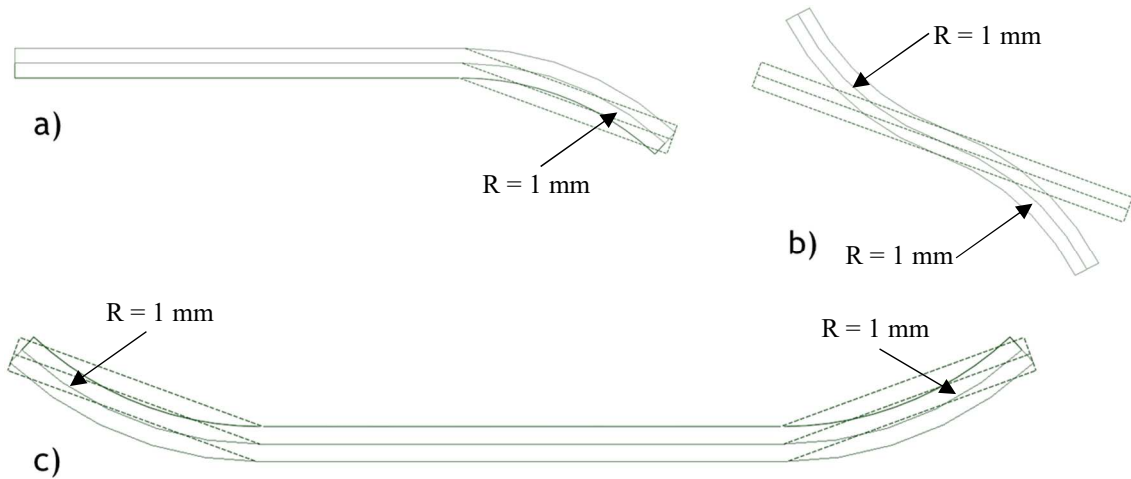


Fig. 3. Curved fin (solid line) interfered with the ordinary flat fin (dash line) at (a) the first (Fin 1) and last (Fin 7) fins, (b) the second (Fin 2), third (Fin 3), fifth (Fin 5), and sixth fins (Fin 6) and (c) the fourth fin (Fin 4).

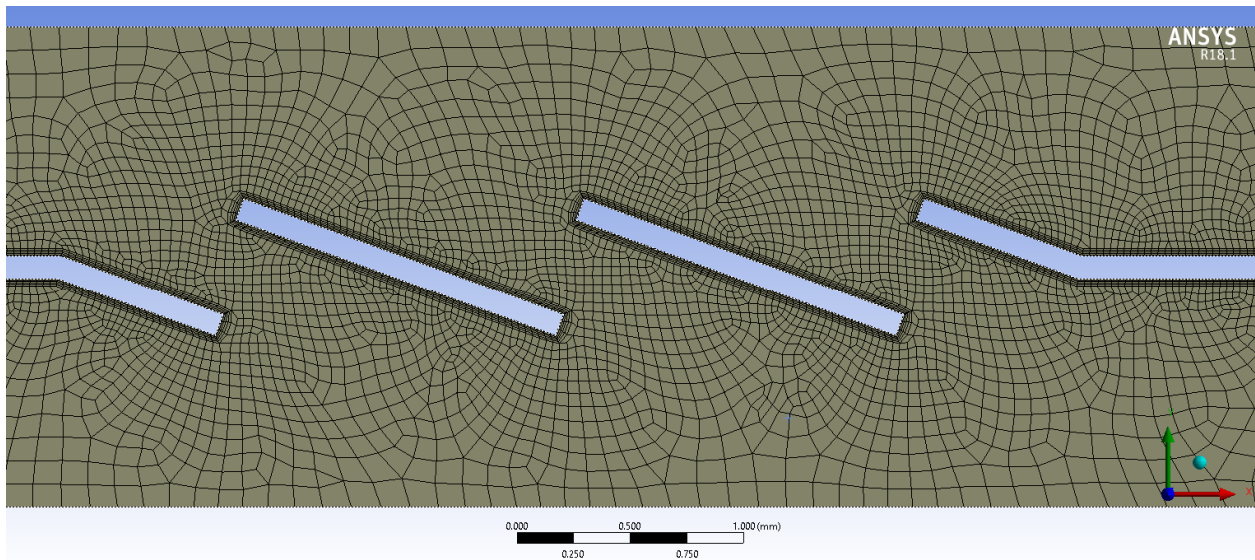


Fig. 4. Meshing result of the medium case.

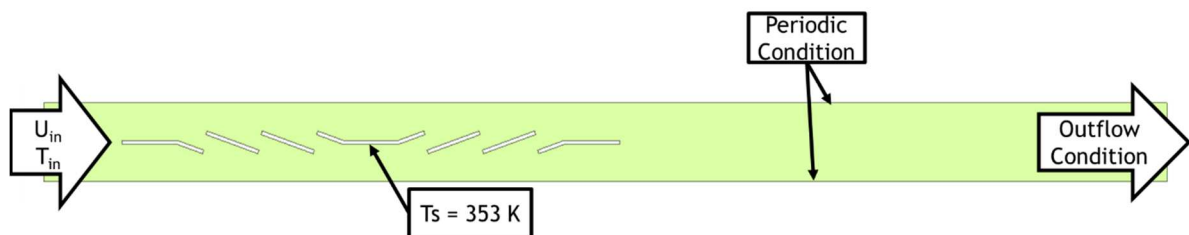


Fig. 5. Boundary conditions.



2.3 Governing Equations

As per Jang and Chen [13], the Reynolds number used in this study was based on the fin pitch (Re_H) ranging from 160 to 1997. This was equivalent to Reynolds number based on the louver pitch (Re_{Lp}) ranging from 133 to 1199. Two effects particularly play an important role in this work: pressure drop of air flowing through the fin domain and heat transfer from fins to airflow. The realizable $k-\epsilon$ was designated to simulate the turbulence flow of this problem. Because heat transfer occurred from the heated wall to the fluid domain, the enhanced wall treatment function was implemented for the near-wall calculation [20]; however, this method required grid configuration at a heated wall controlled by $y^+ < 1$.

The steady-state 2D model was based on the assumptions that airflow was an incompressible flow, and the effects of natural convection and radiation heat transfer were negligible. Moreover, there was no user-defined function applied to this model. Therefore, in this study, the relevant equations used are presented as follows:

Continuity

$$\rho_{air} \nabla \vec{u} = 0 \tag{1}$$

Momentum

$$\rho_{air} \nabla \vec{u} \vec{u} = -\nabla \vec{p} + \mu_{air} \nabla^2 \vec{u} \tag{2}$$

Energy

$$\rho_{air} c_{p,air} \vec{u} \nabla T = k_{air} \nabla^2 T \tag{3}$$

Turbulent kinetic energy (TKE)

$$\rho_{air} \frac{\partial}{\partial x_i} (k_t u_i) = \frac{\partial}{\partial x_j} \left[\left(\mu_{air} + \frac{\mu_t}{\sigma_k} \right) \frac{\partial k_t}{\partial x_j} \right] - \rho_{air} \epsilon \tag{4}$$

Dissipation (ϵ)

$$\rho_{air} \frac{\partial}{\partial x_i} (\epsilon u_i) = \frac{\partial}{\partial x_j} \left[\left(\mu_{air} + \frac{\mu_t}{\sigma_\epsilon} \right) \frac{\partial \epsilon}{\partial x_j} \right] - \rho_{air} C_1 S \epsilon - \rho_{air} \frac{\epsilon^2}{k_t + \sqrt{\nu_{air} \epsilon}} \tag{5}$$

$$C_1 = \max \left[0.43, \frac{\eta}{\eta + 5} \right], \eta = S \frac{k_t}{\epsilon}, S = \sqrt{2 S_{ij} S_{ij}}$$

where ρ_{air} , μ_{air} , $c_{p,air}$, k_{air} , and ν_{air} were density, dynamic viscosity, specific heat capacity, thermal conductivity, and kinematic viscosity of the air, and u , p , T , k , and ϵ were velocity, pressure, temperature, turbulence kinetic energy, and dissipation rate, respectively.

The scale residuals of these equations were set at 10×10^{-9} , except for the energy equation, which was 10×10^{-12} . The SIMPLE method was designated to them. Moreover, a second-order upwind scheme was applied to momentum, energy, TKE, and ϵ terms while a second-order accuracy was obtained for pressure.

2.4 Numerical Calculations

The convective heat transfer can be expressed in term of the average Nusselt number (Nu_H) based on the fin pitch (H) defined as follows:

$$Nu_H = \frac{hH}{k_{air}} \tag{6}$$

h is the average heat transfer coefficient defined as follows:

$$h = \frac{q_{num}}{A_o \Delta T_{lm}} \tag{7}$$

where q_{num} is total heat transfer from fins to airflow, A_o is the total heat transfer area, and ΔT_{lm} is the log-mean temperature difference defined as follows:

$$\Delta T_{lm} = \frac{(T_i - T_w) - (T_o - T_w)}{\ln \left(\frac{T_i - T_w}{T_o - T_w} \right)} \tag{8}$$

where T_o is the air temperature at the outlet.

The average pressure drop across the domain can be expressed in term of Fanning friction factor (f) defined as follows:

$$f = \frac{\Delta P}{\frac{1}{2} \rho U_{in}^2} \cdot \frac{A_c}{A_o} \tag{9}$$

where ΔP is the pressure drop and A_c is the minimum flow area. The parameter used to compare the performance of two fin shapes is the performance evaluation criteria (PEC) defined as follows:

$$PEC = \frac{\left(\frac{Nu}{Nu_{ref}} \right)}{\left(\frac{f}{f_{ref}} \right)^{1/3}} \tag{10}$$



Table 1. Meshing parameters for regulating the number of nodes.

Mesh Solution	Maximum mesh size (mm)	Edge size of the heated wall (mm)	Number of nodes
Coarse	0.2	0.06	6568
Medium	0.15	0.03	16982
Fine	0.1	0.015	41133

where Nu_{ref} and f_{ref} are obtained from the reference (ordinary flat louver fin).

PEC was used for comparing between the effect of heat transfer (represented by Nu) and pressure drop (represented by f) of two heat exchangers. In this study, the new designs were compared to the reference, indicated by PEC, to determine their heat transfer performance.

3. Results and Discussion

3.1 Mesh Number Independence

The reference case (ordinary flat louver fin) was meshed with three parameters shown in Table 1. The Colburn j -factor and Fanning friction factor (f) obtained were validated with the experimental and 3D simulation results of Jang and Chen [13]. However, in this study, we assumed that the flow across the louver fin was 2D as opposed to the 3D model used in [13]. To validate with their experimental and 3D simulation results, the Colburn j -factor and Fanning friction factor (f) were calculated following the equations in their study. They were defined as follows:

$$j = \frac{Nu_H}{Re_H Pr^{1/3}} \quad (11)$$

where Pr is Prandtl number.

$$f_{val} = \frac{\Delta P}{\frac{1}{2} \rho U_{in}^2} \cdot \frac{H}{4L} \quad (12)$$

The comparison of results between this study and the computational and experimental works of Jang and Chen [13] are shown in Figs. 6A and B. The trends in 2D and 3D simulations were similar and were close to the experimental result in the case of Colburn j -factor. However, the Fanning friction factor (f) obtained from the 2D simulation was underpredicted, 15% less than the experimental result. Therefore, the 2D model was valid and thus implemented in this study to save computational time. Fig. 7 shows the independence of results from the mesh number. The maximum difference of the Colburn j -factor between coarse and medium meshes was 12.40% at an inlet velocity of 9 m/s; however, it was 1.95% at an inlet velocity of 8 m/s for medium and fine meshes. Therefore, the maximum size of the mesh, the edge size of the heated wall, and the number of nodes used in this study were 0.15 mm, 0.03 mm, and 16,982, respectively.

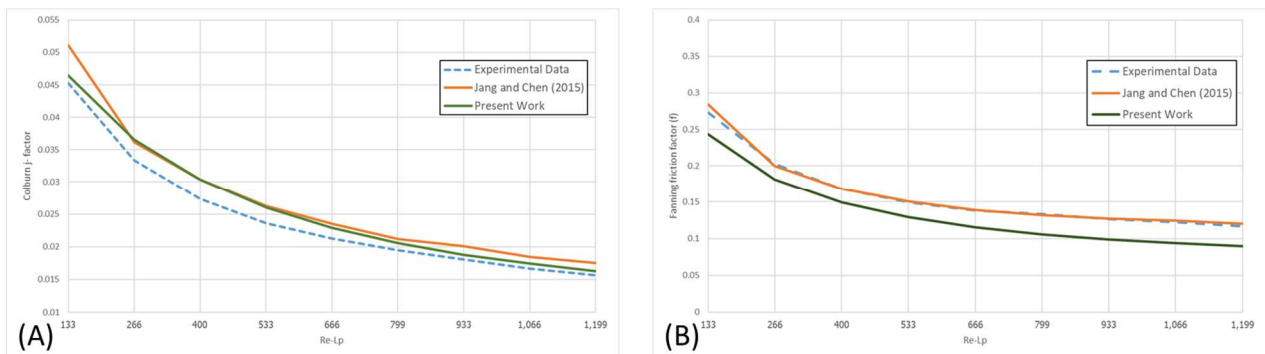


Fig. 6. Validation between simulation and experimental data—the dashed line represents the experimental result from Jang and Chen [13], and solid lines represent 2d simulation results of this study.

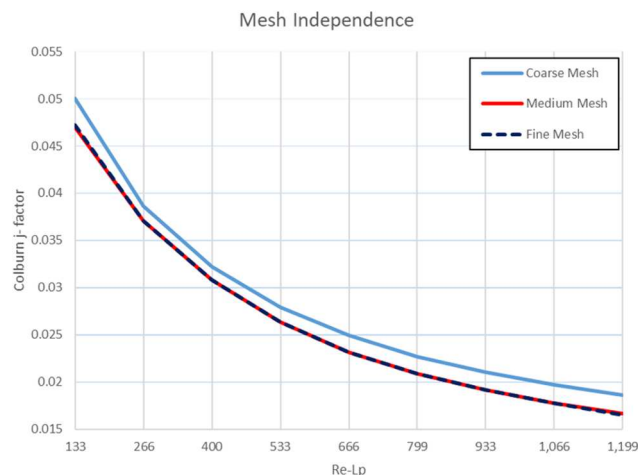


Fig. 7. Mesh independence by comparing Colburn j -factor among three mesh setting—the blue and red solid lines represent the coarse and medium mesh, respectively, and dashed line represents the fine mesh.



3.2 Airflow Velocity Distribution

From the reference case, the location of the maximum flow velocity was on the last fin close to the exit. However, the maximum flow velocity of new designs occurred between fins. Fig. 8 shows the flow velocity contour over different shapes of the fin at an inlet velocity of 1 m/s. The all-curved fin design had a 22.44% maximum velocity increment from that of the reference; its location was between the third and fourth fins. The maximum velocity in other cases increased by 20.03%, 12.81%, and 19.25% for Curves 1-2-3-4-7, 1-2-4-7, and 1-3-4-7, respectively. The locations of shedding vortices differed because of the fins that were curved (Fig. 9). The air velocity at the first half of the fin domain was increased because of these vortices. Moreover, the air temperature at this location was still low because they had traveled for a short time in the fin domain. Therefore, additional heat can be absorbed compared to the reference.

Curved fins created vortices behind themselves. An increase in the local velocity through the curved fins was attributed to these shedding vortices on the fins, as shown in Fig. 9. Air was regulated to flow between fins rather than toward the outlet. Moreover, the air velocity was accelerated by these vortices. This effect enhanced heat transfer; changing the fin structure from the ordinary flat to the curved shape increased the frontal area by 50.39% compared to that of the reference. Figure 10A shows the average Nusselt number (Nu_H) for all cases. All new designs demonstrated heat transfer values more than that of the reference case. However, the vortices increased the pressure drop of the airflow across the fin domain. Figure 10B shows the decrease in Fanning f -factor, which confirmed the previous statement. The more vortices occurred in the fin domain, the larger drop in pressure represented by Fanning f -factor. In this study, the PEC was used to show the performance of MCHXs among the effects of heat transfer and friction. A PEC of >1 showed that the heat gained from using new fin designs could overcome energy dissipation in the form of friction. Figure 10C shows the PEC comparison of new designs. Although the all-curved fin case had a large amount of heat transfer (which was a 37.15% increment from that of the reference at an inlet velocity of 1 m/s), its PEC was the lowest, which was 0.7156 at an inlet velocity of 4 m/s. This was because they had the greatest number of vortices occurring on fins, and therefore afforded a considerable increase in the pressure drop (ΔP) and friction factor (f). However, Curves 1-2-4-7 and 1-3-4-7 resulted in higher PEC than the others, although their Nu values were less than that of the all-curved fin case. Unlike that case, a few vortices took place between fins in Curves 1-2-4-7 and 1-3-4-7. Their pressure drops were, therefore, less than all-curved fin cases. Moreover, their PEC s exceeded that of the all-curved fin case. The highest PEC was possessed by Curve 1-3-4-7, which was 1.15 at an inlet velocity of 1 m/s; however, Curve 1-2-4-7 had a higher PEC at a high inlet velocity ($PEC = 1.01$ at 9 m/s). All new designs had their best performances at 1 m/s; the higher inlet velocity worsened the performance of the heat exchanger.

3.3 Heat Transfer from Fins to Airflow

All cases had seven fins in each flow passage. Each fin had a different amount of heat exchanging to airflow. Figure. 11 shows the percentage of heat transfer from every fin. At a low inlet velocity (1 m/s), the first, third, and fourth fins had high heat transfer percentages. Creating a curved fin decreased the heat transfer from these fins and compensated it at the others. Heat transfer increased at the second fin from 12.45% to 14.80%, 15.53%, and 16.12% for all-curved, Curve 1-2-3-4-7, and Curve 1-2-4-7, respectively, except Curve 1-3-4-7. The difference between Curve 1-3-4-7 and other designs was that there was no vortex at the second fin; however, heat transfer occurred at the fourth fin instead. For the all-curved fin that had the greatest number of vortices in the fin domain, the amount of heat transfer dramatically increased at fifth and sixth fins from 4.03% to 7.64% and 5.33% to 10.98%, respectively. At an intermediate inlet velocity (3 m/s), the heat transfer at the fourth fin significantly decreased from 22.17% (of the reference case) to 15.26%, 15.35%, 19.89%, and 19.28% for the all-curved case, Curves 1-2-3-4-7, 1-2-4-7, and 1-3-4-7, respectively. Unlike the case of low inlet velocity, the distribution of heat transfer at the first three fins did not substantially increase. Moreover, the Nusselt number of all designs demonstrated a small increase at this velocity. Therefore, the effect of rising heat transfer was not enough to overcome the effect of increasing pressure drop, which decreased the PEC to <1 . At a high inlet velocity (7 and 9 m/s), the heat transfer at the fourth fin was the highest owing to high Nusselt number because of greater air velocity than the other velocities, although not as outstanding as for the intermediate inlet velocity. Their heat distribution resembled that of the intermediate inlet velocity but their increasing Nusselt number overcame the effect of increase in pressure drop. Therefore, their PEC values increased with increase in inlet velocity.

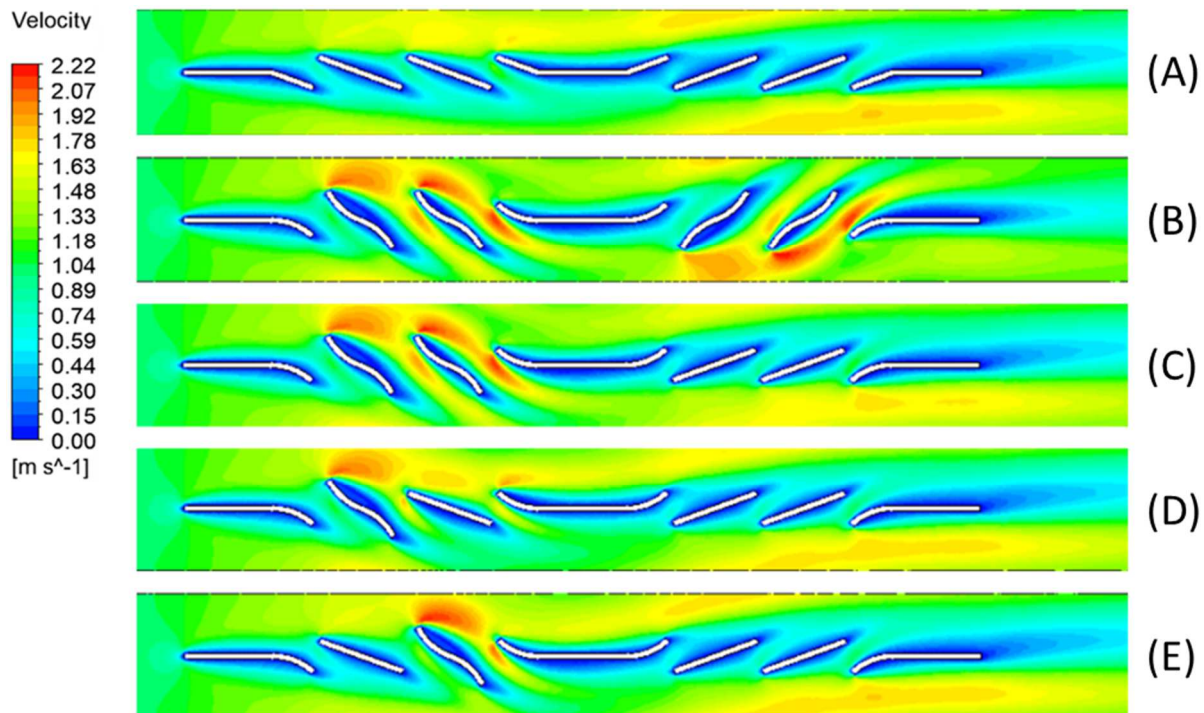


Fig. 8. Velocity contour of different shapes at an inlet velocity of 1 m/s.



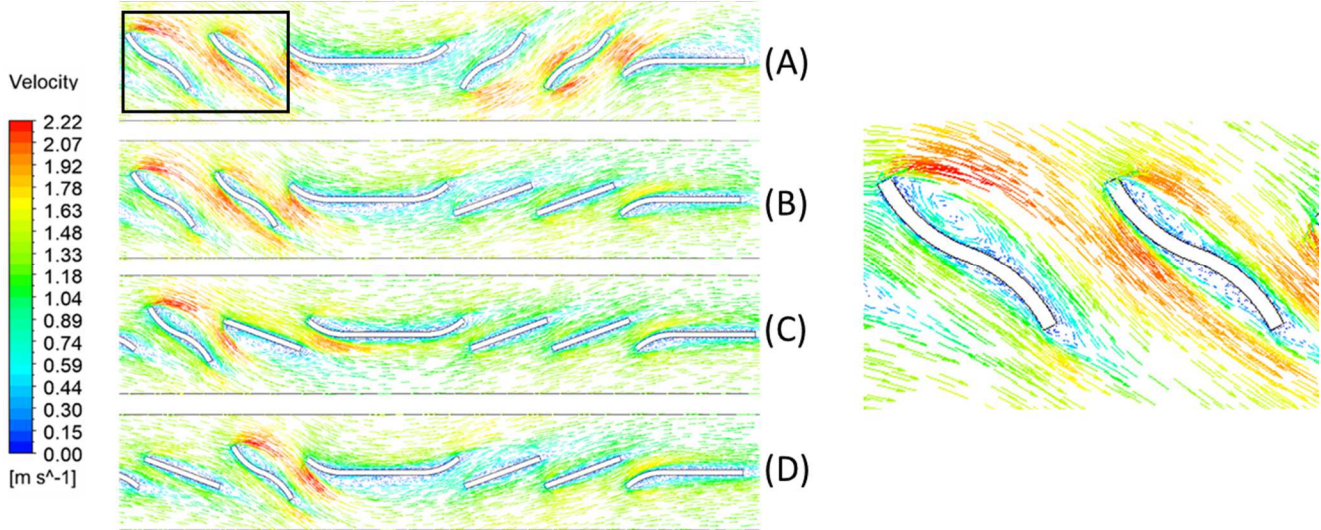


Fig. 9. Vector plot of different shapes at an inlet velocity of 1 m/s with circles indicating the locations of vortices with black circles in the case of (A) All curved, (B) Curve 12347, (C) Curve 1247, and (D) Curve 1347.

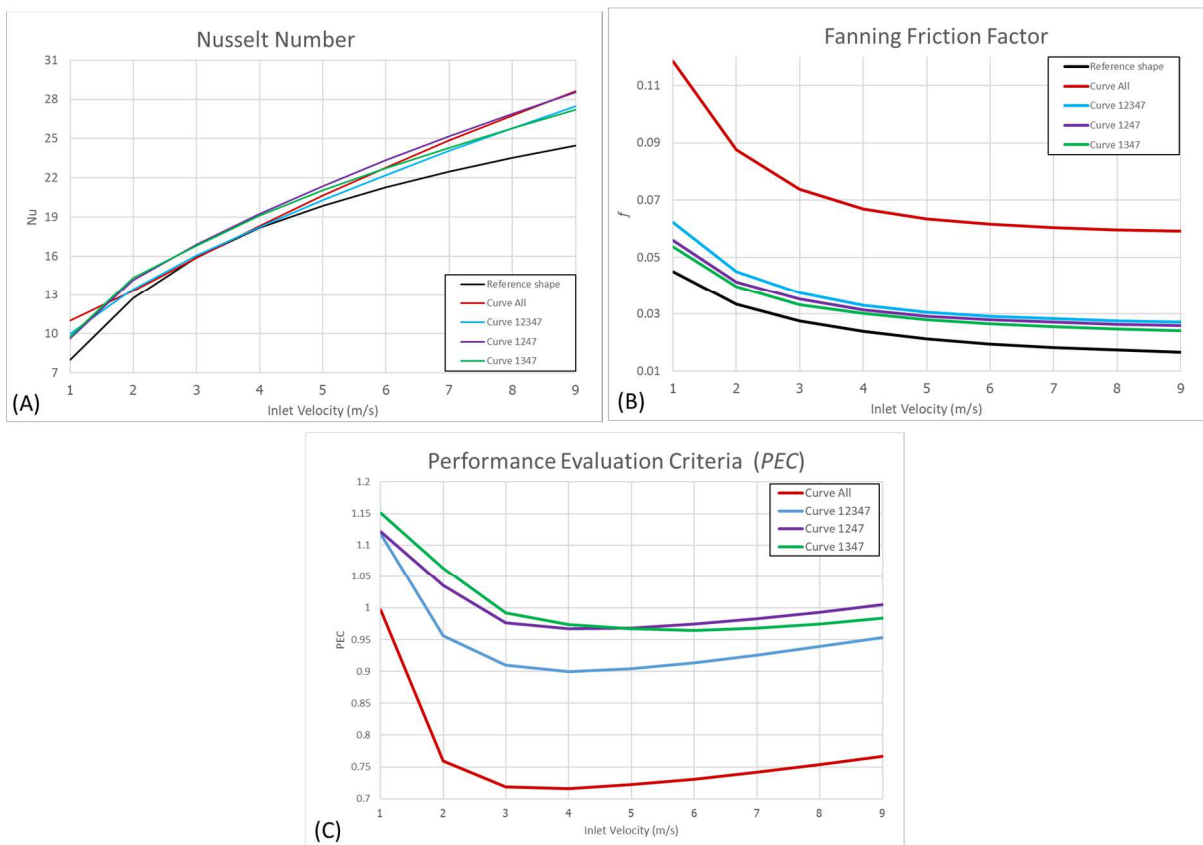


Fig. 10. Calculated results for (A) Nusselt number (Nu_h) and (B) performance evaluation criteria (PEC).

Other parameters such as the number of louver fin and fin angle have not been investigated in this study. Moreover, they require to be optimized based on the effect of increasing heat transfer and friction because of shape alteration. For example, changing the radius of a curved fin increased heat transfer (Fig. 12). For 1.5- and 2.0-mm radii, the heat transfer was enhanced only at a high inlet velocity. However, 0.5- and 0.1-mm radii can increase the Nusselt number at every inlet velocity. These models can be applied to only low inlet velocities and require additional modification for higher inlet velocities.

4. Conclusion

The creation of curved louver fins can enhance heat transfer without adding material to the heat transfer area as the length of each fin was kept constant. The results demonstrated that Curve 1-3-4-7 had the highest PEC (1.15 at 1 m/s), whereas Curve 1-2-4-7 had the best performance at a high inlet velocity (PEC = 1.01 at 9 m/s). The all-curved fin, which had the greatest increment of heat transfer, demonstrated a 37.15% increase from that of the reference at 1 m/s. However, this case was not the best performance as its PEC was below 1 at all the studied inlet velocities. Our observations demonstrated that a change from the ordinary flat to the curved louver fin increased the frontal area, and then created several vortices behind the curved fin. These vortices accelerated air



to flow between fins rather than through the outlet. Therefore, the air was trapped inside for an extended period, resulting in enhanced heat transfer. From the results, this study can be applied to a refrigeration system to increase its efficiency and reduce its operational costs.

Although, curved louver fins can enhance heat transfer, they increase the aerodynamic shape factor, which directly affects flow path and massively increases pressure drop. When air inlet velocity is >3 m/s, the effect of increase in pressure drop overcomes the increase in heat transfer. Hence, the PEC drops and a higher power of the fan or blower is required. For future work, the fin geometries, e.g., its radius of curvature should be improved to generate heat transfer gains without excessively increasing the aerodynamic shape factor.

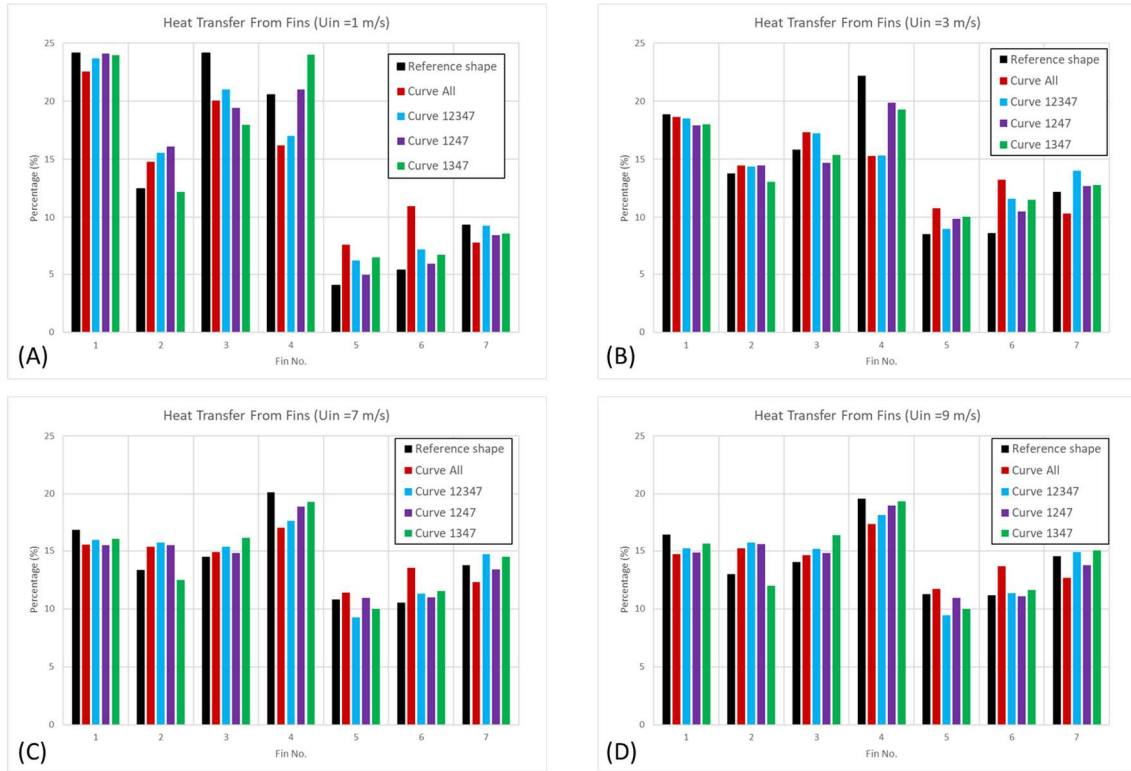


Fig. 11. Amount of heat transfer from fin to airflow at various inlet velocities; (A) 1 m/s, (B) 3 m/s, (C) 7 m/s, and (D) 9 m/s.

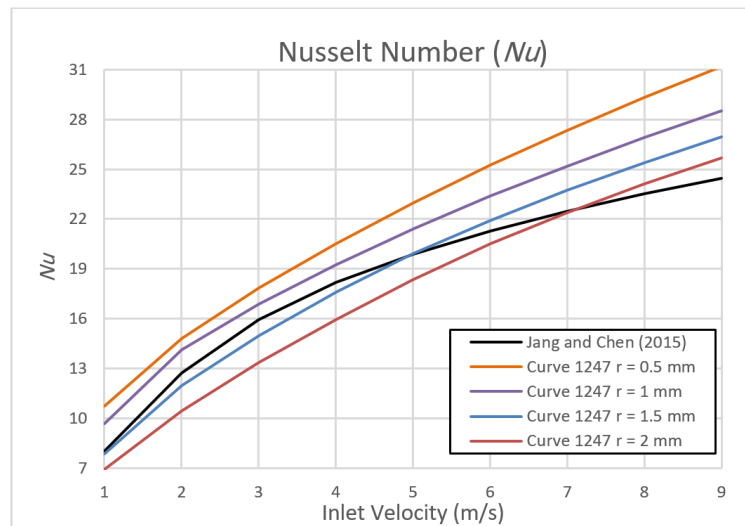


Fig. 12. Variation of curved fin radius in case of 1247.

Author Contributions

K. Wanglertpanich planned the scheme, initiated the project, and analyzed simulation results; P. Siriyothai and T. Hempijid examined validation and conducted the simulations; C. Kittichaikarn supervised the project and analyzed the simulation results. The manuscript was written through the contribution of all authors. All authors discussed the results, reviewed, and approved the final version of the manuscript.



Acknowledgments

The authors would like to thank the Faculty of Engineering, Kasetsart University for a financial support of this work. A support provided by Kasetsart University Research and Development Institute is acknowledged.

Conflict of Interest

The authors declared no potential conflicts of interest concerning the research, authorship, and publication of this article.

Funding

This work was supported by Faculty of Engineering, Kasetsart University, Bangkok, Thailand.

Data Availability Statements

The datasets generated and/or analyzed during the current study are available from the corresponding author on reasonable request.

Nomenclature

A_o	Total Heat Transfer Area [mm ²]	R	Radius [mm]
A_c	Minimum Flow Area [mm ²]	Re	Reynolds Number
CFD	Computational Fluid Dynamics	Re_H	Reynolds Number based on the Fin Pitch
$c_{p,air}$	Air Specific Heat Capacity [$J kg^{-1} K^{-1}$]	Re_{Lp}	Reynolds Number based on the Louver Pitch
f	Fanning Friction Factor	t	Fin Thickness [mm]
h	Average Heat Transfer Coefficient [$W m^{-2} K^{-1}$]	T_i	Inlet Temperature [K]
H	Fin Pitch [mm]	T_{lm}	Log-mean Temperature [K]
j	Colburn j-factor	T_o	Outlet Temperature [K]
k_{air}	Air Thermal Conductivity [$W m^{-1} K^{-1}$]	T_w	Fin Surface Temperature [K]
k_t	Air Turbulent Kinetic Energy [$m^2 s^{-2}$]	u	Velocity [$m s^{-1}$]
L	Flow Passage Length [mm]	U_{in}	Inlet Flow Velocity [$m s^{-1}$]
L_p	Louver Pitch [mm]	y^+	First Layer thickness
MCHXs	Microchannel Heat Exchangers	ϵ	Dissipation Rate of the TKE of the $k-\epsilon$ Model [$m^2 s^{-3}$]
Nu_H	Average Nusselt Number based on the Fin Pitch	ϑ	Louver Angle [degree]
p	Pressure [Pa]	$\Delta\vartheta$	Louver Variable Angle [degree]
PEC	Performance Evaluation Criteria	μ_{air}	Air Dynamic Viscosity [$kg m^{-1} s^{-1}$]
Pr	Prandtl Number	ρ_{air}	Air Density [$kg m^{-3}$]
q_{num}	Total Heat Transfer from Fins to Airflow [W]		

References

- [1] Mori Y., Nakayama W., Recent advances in compact heat exchangers in Japan, COMPACT HEAT EXCHANGERS-HISTORY, TECHNOLOGICAL ADVANCEMENT & MECHANICAL DESIGN PROBLEMS, ASME WINTER ANNUAL MEETING, 10, 1980, 5-16.
- [2] Rohsenow W.M., Hartnett J.P., Ganic E.N., *Handbook of heat transfer applications*, New York, McGraw-Hill Book Co., 1985.
- [3] Webb R.L., Trauger P., How structure in the louvered fin heat exchanger geometry, *Experimental Thermal and Fluid Science*, 4(2), 1991, 205-217.
- [4] Chang Y.J., Wang C.C., A generalized heat transfer correlation for louver fin geometry, *International Journal of Heat and Mass Transfer*, 40(3), 1997, 533-544.
- [5] Wang C.C., Lee C.J., Chang C.T., Lin S.P., Heat transfer and friction correlation for compact louvered fin-and-tube heat exchangers, *International Journal of Heat and Mass Transfer*, 42(11), 1999, 1945-1956.
- [6] Chang Y.J., Hsu K.C., Lin Y.T., Wang C.C., A generalized friction correlation for louver fin geometry, *International Journal of Heat and Mass Transfer*, 43(12), 2000, 2237-2243.
- [7] Park Y.G., Jacobi A.M., Air-Side Heat Transfer and Friction Correlations for Flat-Tube Louver-Fin Heat Exchangers, *Journal of Heat Transfer*, 131(2), 2008, 021801-021801-12.
- [8] Kim M.H., Bullard C.W., Air-side thermal hydraulic performance of multi-louvered fin aluminum heat exchangers, *International Journal of Refrigeration*, 25(3), 2002, 390-400.
- [9] Shah R.K., Sekulic D.P., *Fundamentals of heat exchanger design*, John Wiley & Sons, 2003.
- [10] Sadeghianjahromi A., Kheradmand S., Nemati H., Developed correlations for heat transfer and flow friction characteristics of louvered finned tube heat exchangers, *International Journal of Thermal Sciences*, 129, 2018, 135-144.
- [11] Perrotin T., Clodic D., Thermal-hydraulic CFD study in louvered fin-and-flat-tube heat exchangers, *International Journal of Refrigeration*, 27(4), 2004, 422-432.
- [12] Ryu K., Yook S.J., Lee K.S., Optimal design of a corrugated louvered fin, *Applied Thermal Engineering*, 68(1), 2014, 76-79.
- [13] Jang J.Y., Chen C.C., Optimization of louvered-fin heat exchanger with variable louver angles, *Applied Thermal Engineering*, 91, 2015, 138-150.
- [14] Qian Z., Wang Q., Cheng J., Deng J., Simulation investigation on inlet velocity profile and configuration parameters of louver fin, *Applied Thermal Engineering*, 138, 2018, 173-182.
- [15] Tanaka T., Itoh M., Kudoh M., Tomita A., Improvement of Compact Heat Exchangers with Inclined Louvered Fins, *Bulletin of JSME*, 27(224), 1984, 219-226.
- [16] Manglik R.M., Bergles A.E., Heat transfer and pressure drop correlations for the rectangular offset strip fin compact heat exchanger, *Experimental Thermal and Fluid Science*, 10(2), 1995, 171-180.
- [17] Dejong N.C., Jacobi A.M., An experimental study of flow and heat transfer in parallel-plate arrays: local, row-by-row and surface average behavior, *International Journal of Heat and Mass Transfer*, 40(6), 1997, 1365-1378.
- [18] Wanglertpanich K., Kittichaikarn C., Heat transfer efficiency enhancement using zigzag louvered fin, *Numerical Heat Transfer, Part A: Applications*, 79(4), 2021, 278-293.
- [19] ANSYS FLUENT 18.1 Theory Guide, 2017.



ORCID iD

Kiatbodin Wanglertpanich  <https://orcid.org/0000-0003-0997-9545>

Patcharakon Siriyothai  <https://orcid.org/0000-0003-1254-8586>

Thanathorn Hempijid  <https://orcid.org/0000-0003-3496-1793>

Chawalit Kittichaikarn  <https://orcid.org/0000-0003-2991-8045>



© 2022 Shahid Chamran University of Ahvaz, Ahvaz, Iran. This article is an open access article distributed under the terms and conditions of the Creative Commons Attribution-NonCommercial 4.0 International (CC BY-NC 4.0 license) (<http://creativecommons.org/licenses/by-nc/4.0/>).

How to cite this article: Wanglertpanich K., Siriyothai P., Hempijid T., Kittichaikarn C. A Study of Curved Louver Fin Configuration for Heat Transfer Enhancement, *J. Appl. Comput. Mech.*, 8(2), 2022, 754–763.
<https://doi.org/10.22055/JACM.2022.38042.3136>

Publisher's Note Shahid Chamran University of Ahvaz remains neutral with regard to jurisdictional claims in published maps and institutional affiliations.

